

# Effects of corneal thickness distribution and apex position on postoperative refractive status after full-bed deep anterior lamellar keratoplasty<sup>\*</sup>

Bing-hong WANG, Ye-sheng XU, Wen-jia XIE, Yu-feng YAO<sup>†‡</sup>

Department of Ophthalmology, Sir Run Run Shaw Hospital, Zhejiang University School of Medicine, Hangzhou 310016, China

<sup>†</sup>E-mail: yaoyf@zju.edu.cn

Received Apr. 15, 2018; Revision accepted July 12, 2018; Crosschecked Oct. 22, 2018

**Abstract:** Objective: To investigate the effects of corneal thickness distribution and apex position on postoperative refractive status after full-bed deep anterior lamellar keratoplasty (FBDALK). Methods: This is a retrospective analysis of patients who were diagnosed with advanced keratoconus between 2011 and 2014 in our hospital. The base of the cone in all patients did not exceed the central cornea at a 6-mm range. The FBDALK was performed by a same surgeon. All patients had a complete corneal suture removal and the follow-up records were intact. Patients who had graft-bed misalignment or who were complicated with a cataract or glaucoma were excluded. Uncorrected visual acuity (UCVA), best spectacle corrected visual acuity (BSCVA), and Pentacam examination data were recorded at two years postoperatively. The recorded data included the superior-inferior (S-I) and nasal-temporal (N-T) corneal thickness differences in 2, 4, 6, and 8 mm diameter concentric circles with the corneal apex as the center ( $S-I_{2\text{ mm}}$ ,  $S-I_{4\text{ mm}}$ ,  $S-I_{6\text{ mm}}$ ,  $S-I_{8\text{ mm}}$ ,  $N-T_{2\text{ mm}}$ ,  $N-T_{4\text{ mm}}$ ,  $N-T_{6\text{ mm}}$ , and  $N-T_{8\text{ mm}}$ ), the linear, X-axis, and Y-axis distance between the corneal pupillary center and the cornea apex, total corneal astigmatism at a zone of 3 mm diameter from the corneal apex ( $TA_{3\text{ mm}}$ ), the astigmatic vector values  $J_0$  and  $J_{45}$ , and the corneal total higher-order aberration for 3 and 6 mm pupil diameters ( $HOA_{3\text{ mm}}$  and  $HOA_{6\text{ mm}}$ ). Statistical analysis was performed by SPSS 15.0. Results: A total of 47 eyes of 46 patients met the criteria and were included in this study. The mean follow-up time was (28±7) months. The mean UCVA was 0.45±0.23 (logMAR) (MAR: minimum angle of resolution) and the mean BSCVA was 0.19±0.15 (logMAR), which were all significantly positively correlated with postoperative  $TA_{3\text{ mm}}$  and  $HOA_{3\text{ mm}}$ . The mean S-I corneal thickness differences were (44.62±37.74)  $\mu\text{m}$ , and the mean N-T was (38.57±32.29)  $\mu\text{m}$ .  $S-I_{2\text{ mm}}$  was significantly positively correlated with  $J_0$  ( $r=0.31$ ),  $J_{45}$  ( $r=0.42$ ),  $HOA_{3\text{ mm}}$  ( $r=0.37$ ), and  $HOA_{6\text{ mm}}$  ( $r=0.48$ ).  $S-I_{4\text{ mm}}$  and  $S-I_{8\text{ mm}}$  were significantly positively correlated with  $HOA_{3\text{ mm}}$  ( $r=0.30$ ,  $r=0.40$ ) and  $HOA_{6\text{ mm}}$  ( $r=0.46$ ,  $r=0.35$ ). The X-axis distance between corneal pupillary center and corneal apex was significantly positively correlated with  $J_{45}$  ( $r=0.29$ ). Conclusions: In patients with advanced keratoconus after FBDALK, the unevenly distributed thickness at corneal pupillary area and the misalignment of corneal apex and pupillary center might cause significant regular and irregular astigmatism, which affected the postoperative visual quality.

**Key words:** Full-bed deep anterior lamellar keratoplasty; Corneal thickness distribution; Corneal apex  
<https://doi.org/10.1631/jzus.B1800230>

**CLC number:** R779.65

## 1 Introduction

<sup>‡</sup> Corresponding author

\* Project supported by the Medical Scientific Research Foundation of Zhejiang Province (No. 2018ZD007), China

ORCID: Yu-feng YAO, <https://orcid.org/0000-0003-1494-9711>

© Zhejiang University and Springer-Verlag GmbH Germany, part of Springer Nature 2018

Optical keratoplasty includes penetrating keratoplasty, deep anterior lamellar keratoplasty, and Descemet's membrane exposure full-bed deep anterior lamellar keratoplasty (FBDALK) (Yao et al.,

2002; Yao, 2008; Bonci et al., 2011; Wu et al., 2012; Zhang et al., 2013; Javadi et al., 2014). The purpose of surgery is to restore the patient's visual function as much as possible. In addition to focusing on the transparency of the cornea, attention should also be given to the refractive status of the surgical eye, especially for astigmatism. High astigmatism or irregular astigmatism will significantly affect postoperative visual acuity; some patients even had uncorrectable low vision due to the astigmatism (Serdarevic, 1994; Sarhan et al., 2000; Vajpayee et al., 2001; Javadi et al., 2011; Fares et al., 2012b). It has been reported that 29.3% of the keratoconic patients after penetrating keratoplasty had an astigmatism over four diopters (Javadi et al., 2005), while 28.0% of the keratoconic patients after FBDALK had an astigmatism over five diopters (Zhang et al., 2013).

Factors that contribute to postoperative astigmatism or irregular astigmatism include: suture technique, removal and adjustment of sutures; type of trephine, oval or eccentric trephining; curvature, alignment, size, shape, thickness, and apex position shift of the graft and bed (Serdarevic, 1994; Sarhan et al., 2000; Vajpayee et al., 2001; Javadi et al., 2011; Fares et al., 2012b; Espandar et al., 2016). Many relevant studies have been reported on the aforementioned factors except the bias of the thickness and apex position of the graft and bed.

The Pentacam anterior segment analysis system is based on the Scheimpflug imaging principle. A 360° rotating measurement probe is used to scan the anterior segment of the eye for simultaneous acquisition of corneal thickness at any point, as well as the corneal apex and corneal pupillary center. In addition, corneal astigmatism at a certain distance from the apex and corneal higher-order aberrations at each pupil diameter can all be detected, i.e., the Pentacam anterior segment analysis system can quantitatively analyze the regular and irregular astigmatism in the cornea. The method also has the advantages of high data accuracy, good repeatability, non-contact, short examination time, and easy acceptance by the patients (Uçakhan et al., 2006; Shankar et al., 2008; Ponce et al., 2009; Nam et al., 2010; Bae et al., 2014; Özyol and Özyol, 2016).

Therefore, we used a Pentacam anterior segment analysis system to investigate the effects of corneal thickness distribution and the apex position after

FBDALK on postoperative refractive status in keratoconic eyes.

## 2 Methods

### 2.1 Inclusion and exclusion criteria

Inclusion criteria: (1) from 2011 to 2014, the diagnosis of keratoconus (advanced stage) in our hospital and the base of cone did not exceed 6 mm of the central cornea; (2) the FBDALK was performed by the same surgeon and the surgery was uneventful, Descemet's membrane was completely exposed during surgery, and no postoperative complications occurred; (3) corneal sutures have been completely removed; (4) regular follow-up, and follow-up data were intact. Consecutive cases that met all of the above conditions were included in this study. Exclusion criteria: (1) combined with strabismus or amblyopia, glaucoma, retinal disease, or other ocular diseases; (2) had other ocular surgeries prior or after the FBDALK; (3) anterior segment optical coherence tomography (AS-OCT) examination found graft-bed alignment abnormalities such as step-like incision, sulcus or local bulge-like changes. This study was a retrospective, non-control case study.

### 2.2 Surgical techniques

All FBDALK procedures were performed by the same experienced surgeon (YF YAO). After general anesthesia, the superior and inferior recti were traction-fixed. To align the pupil as the center, a sharp trephine was used to mark the bed demarcation on the corneal surface and then cut to 2/3 corneal thickness. A gem knife was used to separate the anterior-middle stroma from the rest of the stroma at 12 o'clock. A pair of specific forceps (Yao, 2008) was used to hook the posterior stromal fibers, and a 27-gauge cannula with beveled tip was inserted into the posterior stromal fibers and injected a few viscoelastic agent; then a small amount of air was injected to form a layer of honeycomb bubble in the same layer of stroma, a blunt-tip 27-gauge cannula was replaced to gradually separate the first layer of lamella using blunt or viscoelastic dissection, and the stroma was removed along the cut edge. A 1-ml syringe was used to extract a small amount of aqueous humor at the limbus. A larger bubble was sought between the residual stroma

and the Descemet's membrane, forceps were used to hook a small pocket, a viscoelastic agent was inserted, and the stroma was separated and removed with blunt or viscoelastic dissection to completely expose the Descemet's membrane. We took a cryopreserved eye to make a donor button with sharp trephine, and the pupil was aligned as the center. We placed and aligned the graft on the recipient bed, sewn 10-0 nylon interrupt sutures at the superior, inferior, nasal, and temporal cornea to form a square pattern, and then symmetrically sutured the graft with a total of 16 bites of interrupted sutures, then adjusted the tightness and embedded the suture knot. Tobradex eye ointment was applied into the conjunctival sac, and the eye was covered by gauze and goggle patches. Both the graft and bed sizes ranged from 7.5 to 8.0 mm, and the graft was larger than the bed by 0.25–0.50 mm in each case.

### 2.3 Postoperative follow-up

Fluorometholone eye drops (0.1%, Santen Pharmaceutical Co., Osaka, Japan) and ofloxacin eye ointment (Santen Pharmaceutical Co., Osaka, Japan) were used routinely for anti-inflammatory anti-infection treatment for six months. A detailed clinical examination was performed at every visit, including slit lamp examination, refraction, Pentacam, and AS-OCT. Sutures were removed according to the tightness at six months after surgery, and all the sutures were removed around one and a half years after surgery. The uncorrected visual acuity (UCVA), best spectacle corrected visual acuity (BSCVA), and Pentacam anterior segment analysis system results (Pentacam HR, Oculus, Germany) were recorded at two years after surgery. Pentacam examinations were performed by skilled technicians, and each eye was measured three times. The unqualified results were excluded, and the results with relatively good reproducibility were selected as final statistical parameters. The recorded data included: (1) corneal thickness at superior, inferior, nasal and temporal areas in 2, 4, 6, and 8 mm diameter concentric circles with the corneal apex as the center ( $CT_{2\text{ mm}}$ ,  $CT_{4\text{ mm}}$ ,  $CT_{6\text{ mm}}$ ,  $CT_{8\text{ mm}}$ ). The superior-inferior (S-I) and nasal-temporal (N-T) corneal thickness differences were calculated and recorded as  $S-I_{2\text{ mm}}$ ,  $S-I_{4\text{ mm}}$ ,  $S-I_{6\text{ mm}}$ ,  $S-I_{8\text{ mm}}$  and  $N-T_{2\text{ mm}}$ ,  $N-T_{4\text{ mm}}$ ,  $N-T_{6\text{ mm}}$ ,  $N-T_{8\text{ mm}}$ , respectively. The corneal apex is the highest point of the cornea under fixation. (2) Total corneal astigmatism at a zone of 3 mm diameter from the corneal apex ( $TA_{3\text{ mm}}$ ) was recorded,

and the astigmatic vector values  $J_0$  and  $J_{45}$  were calculated using the following equations:

$$J_0 = -C/2 \times \cos 2a, \quad (1)$$

$$J_{45} = -C/2 \times \sin 2a, \quad (2)$$

where  $C$  is the power of cylinder,  $a$  is the axis of cylinder,  $J_0$  is the cylindrical power at  $90^\circ$  or  $180^\circ$  meridian, and  $J_{45}$  is the cylindrical power at  $45^\circ$  or  $135^\circ$  meridian. (3) The linear,  $X$ -axis, and  $Y$ -axis distance between the corneal pupillary center and the cornea apex. (4) The corneal total higher-order aberration for 3 and 6 mm pupil diameters ( $HOA_{3\text{ mm}}$  and  $HOA_{6\text{ mm}}$ ).

### 2.4 Statistical analysis

The Statistical Package for Social Sciences (SPSS Version 15.0; Cary, NC, USA) was used to perform statistical analysis. One-way analysis of variance (ANOVA) was used to compare and analyze the differences between groups. The significance level was set to  $P < 0.05$ .

## 3 Results

### 3.1 General characteristics

From 2011 to 2014, a total of 130 eyes diagnosed as keratoconus (advanced stage) underwent FBDALK, which was successfully performed by the same surgeon at our department. During surgery, Descemet's membrane was completely exposed and no postoperative complications occurred. Among 130 eyes, 55 eyes had complete Pentacam and the other examinations during the follow-up of about two years. Among 55 eyes, one case had glaucoma, one case had amblyopia, and one case had the cone base exceeding 6 mm of central cornea. AS-OCT examination showed that there were five cases of step-like, sulcus, or local bulge-like changes, which were excluded. The remaining 47 eyes (9 females, 38 males) of 46 cases were included in this study, with an average age of  $(23.0 \pm 4.80)$  years and an average follow-up time of  $(28 \pm 7)$  months.

### 3.2 Correlations between UCVA, BSCVA and TA, HOA

Table 1 shows the patients' UCVA, BSCVA,  $TA_{3\text{ mm}}$ ,  $HOA_{3\text{ mm}}$ , and  $HOA_{6\text{ mm}}$ . There were significant

positive correlations between UCVA (logMAR), BSCVA (logMAR) and TA<sub>3 mm</sub>; the correlation coefficients were 0.4 and 0.5, respectively. There was a significant positive correlation between UCVA (logMAR) and HOA<sub>3 mm</sub> with a correlation coefficient of 0.31 (Table 2). This indicated that the higher the power of corneal astigmatism, the higher the degree of HOA and the worse the patient's vision after FBDALK in keratoconic eyes.

### 3.3 Corneal thickness at different positions

The mean thickness of the corneal apex was (488.00±41.12) μm. Corneal thickness at different

concentric circles at superior, inferior, nasal, and temporal cornea is shown in Table 3 and Fig. 1. Significant differences in corneal thickness at 2, 4, and 6 mm diameter concentric circles were found between all regions, while no significant difference was found at 8 mm. In all subjects, the sizes of the graft and bed ranged from 7.5 to 8.0 mm; therefore, the thickness of the 6 mm ring was the thickness of the graft. The thickness of the 8 mm ring might be the thickness of the graft-bed junction. The results suggested that there might be significant differences in the thickness of the graft at each diameter concentric circle, but not in the thickness of the bed.

### 3.4 Correlations between corneal thickness differences, apex position and TA, HOA

The S-I<sub>2 mm</sub>, S-I<sub>4 mm</sub>, S-I<sub>6 mm</sub>, and S-I<sub>8 mm</sub> were (33.57±26.42), (44.77±39.14), (47.45±37.14), and (52.89±44.49) μm, respectively, with an average of (44.62±37.74) μm. The N-T<sub>2 mm</sub>, N-T<sub>4 mm</sub>, N-T<sub>6 mm</sub>, and N-T<sub>8 mm</sub> were (28.15±19.46), (35.23±29.61), (39.23±34.50), and (51.66±38.68) μm, respectively, with an average of (38.57±32.29) μm. The linear, X-axis, and Y-axis distance from the pupillary center to the corneal apex were (0.47±0.23), (0.25±0.20), and (0.34±0.25) mm, respectively.

The correlations between S-I and N-T corneal thickness differences, the linear, X-axis, and Y-axis distances and TA<sub>3 mm</sub>, vectors J<sub>0</sub> and J<sub>45</sub>, HOA<sub>3 mm</sub>, HOA<sub>6 mm</sub> are shown in Table 4. Among them, S-I<sub>2 mm</sub>

**Table 1** UCVA, BSCVA, astigmatism, and HOA in keratoconic patients after FBDALK

Variable	Value
Spherical power (D)	1.49±3.87
Cylindrical power (D)	-4.62±2.56
Spherical equivalent (D)	-0.78±3.68
UCVA (logMAR)	0.43±0.23
BSCVA (logMAR)	0.18±0.15
TA <sub>3 mm</sub> (D)	5.00±2.80
J <sub>0</sub> (D)	0.00±2.40
J <sub>45</sub> (D)	0.00±1.90
HOA <sub>3 mm</sub>	0.39±0.19
HOA <sub>6 mm</sub>	2.53±1.12

Data are expressed as mean±standard deviation (*n*=47); D, diopters; MAR, minimum angle of resolution; UCVA, uncorrected visual acuity expressed; BSCVA, best spectacle corrected visual acuity expressed; TA<sub>3 mm</sub>, total corneal astigmatism at 3 mm of corneal apex; HOA<sub>3 mm</sub>, corneal total higher-order aberration at 3 mm pupil diameter; HOA<sub>6 mm</sub>, corneal total higher-order aberration at 6 mm pupil diameter

**Table 2** Correlations between UCVA, BSCVA and TA<sub>3 mm</sub>, J<sub>0</sub>, J<sub>45</sub>, HOA<sub>3 mm</sub>, HOA<sub>6 mm</sub> in keratoconic patients after FBDALK (*n*=47)

Variable	TA <sub>3 mm</sub>		J <sub>0</sub>		J <sub>45</sub>		HOA <sub>3 mm</sub>		HOA <sub>6 mm</sub>	
	r	Sig.	r	Sig.	r	Sig.	r	Sig.	r	Sig.
UCVA	0.40	0.00*	0.04	0.80	-0.11	0.45	0.31	0.03*	0.15	0.33
BSCVA	0.50	0.00*	0.25	0.09	-0.02	0.89	0.17	0.27	0.10	0.52

\* Pearson correlation, significant (Sig.) at the 0.05 level. UCVA, uncorrected visual acuity expressed; BSCVA, best spectacle corrected visual acuity expressed; TA<sub>3 mm</sub>, total corneal astigmatism at 3 mm from corneal apex; J<sub>0</sub>, cylindrical power at 90° or 180° meridian; J<sub>45</sub>, cylindrical power at 45° or 135° meridian; HOA<sub>3 mm</sub>, corneal total higher-order aberration at 3 mm pupil diameter; HOA<sub>6 mm</sub>, corneal total higher-order aberration at 6 mm pupil diameter

**Table 3** Corneal thickness in each diameter concentric circles and the difference *P* values between superior, inferior, nasal, and temporal areas in keratoconic patients after FBDALK

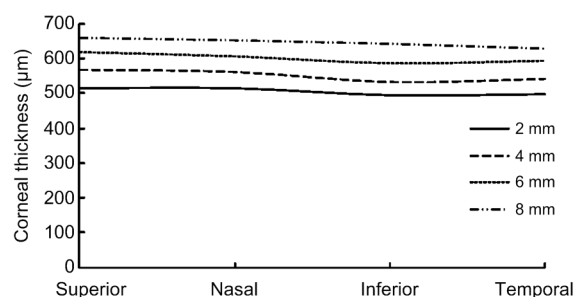
Diameter (mm)	Corneal thickness (μm)					<i>P</i> value
	Superior	Inferior	Nasal	Temporal	Mean	
2	515±45	495±44	515±41	498±43	495±40	0.03*
4	568±48	533±47	562±42	542±46	540±39	0.00*
6	619±52	587±54	607±53	594±57	589±45	0.02*
8	660±79	643±74	653±76	629±70	633±61	0.20
Mean	547±68	565±79	584±75	565±74		

Data are expressed as mean±standard deviation (*n*=47). \* One-way ANOVA, significant at the 0.05 level

**Table 4** Correlations between the corneal thickness differences, pupillary center position and TA,  $J_0$ ,  $J_{45}$ , HOA in keratoconic patients after FBDALK ( $n=47$ )

Variable	TA <sub>3 mm</sub>		$J_0$		$J_{45}$		HOA <sub>3 mm</sub>		HOA <sub>6 mm</sub>	
	r	Sig.	r	Sig.	r	Sig.	r	Sig.	r	Sig.
Corneal thickness difference										
S-I <sub>2 mm</sub>	0.27	0.07	0.31	0.03*	0.42	0.00*	0.37	0.01*	0.48	0.00*
S-I <sub>4 mm</sub>	0.25	0.09	0.21	0.15	0.28	0.06	0.30	0.04*	0.46	0.00*
S-I <sub>6 mm</sub>	0.25	0.09	0.27	0.07	0.14	0.35	0.28	0.06	0.54	0.00*
S-I <sub>8 mm</sub>	0.05	0.74	0.19	0.20	-0.07	0.65	0.40	0.01*	0.35	0.01*
N-T <sub>2 mm</sub>	-0.12	0.43	-0.23	0.13	-0.16	0.30	0.08	0.60	0.03	0.86
N-T <sub>4 mm</sub>	-0.09	0.56	-0.08	0.61	-0.02	0.88	0.04	0.78	0.12	0.43
N-T <sub>6 mm</sub>	-0.09	0.54	-0.05	0.72	0.13	0.38	0.18	0.23	0.19	0.20
N-T <sub>8 mm</sub>	-0.06	0.66	-0.11	0.47	-0.05	0.73	0.15	0.33	-0.05	0.76
Distance from pupillary center to corneal apex										
Lineal distance	-0.01	0.94	0.17	0.26	0.03	0.84	0.07	0.63	0.24	0.10
X-axis distance	0.06	0.70	-0.05	0.73	0.29*	0.05	-0.01	0.95	0.21	0.15
Y-axis distance	-0.05	0.76	-0.01	0.92	-0.03	0.86	-0.21	0.15	-0.11	0.45

\* Pearson correlation, significant (Sig.) at the 0.05 level. S-I<sub>2 mm</sub>, S-I<sub>4 mm</sub>, S-I<sub>6 mm</sub>, S-I<sub>8 mm</sub>: superior-inferior corneal thickness differences at 2, 4, 6, and 8 mm diameter concentric circles from the corneal apex, respectively; N-T<sub>2 mm</sub>, N-T<sub>4 mm</sub>, N-T<sub>6 mm</sub>, N-T<sub>8 mm</sub>: nasal-temporal corneal thickness differences at 2, 4, 6, and 8 mm diameter concentric circles from the corneal apex, respectively; TA<sub>3 mm</sub>: total corneal astigmatism at 3 mm from the corneal apex;  $J_0$ : cylindrical power at 90° or 180° meridian;  $J_{45}$ : cylindrical power at 45° or 135° meridian; HOA<sub>3 mm</sub>: corneal total higher-order aberration at 3 mm pupil diameter; HOA<sub>6 mm</sub>: corneal total higher-order aberration at 6 mm pupil diameter

**Fig. 1** Corneal thickness curves of superior, inferior, nasal, and temporal areas in keratoconic patients after FBDALK

and corneal astigmatism vectors  $J_0$  and  $J_{45}$ , HOA<sub>3 mm</sub>, and HOA<sub>6 mm</sub> had significant positive correlations; the correlation coefficients were 0.31, 0.42, 0.37, and 0.48, respectively. S-I<sub>4 mm</sub> and S-I<sub>8 mm</sub> had significant positive correlations with HOA<sub>3 mm</sub> ( $r=0.30$ ,  $r=0.40$ ) and HOA<sub>6 mm</sub> ( $r=0.46$ ,  $r=0.35$ ). The X-axis distance from corneal apex to the corneal pupillary center had significant positive correlation with corneal astigmatism vector  $J_{45}$  ( $r=0.29$ ). However, there was no significant correlation between the difference of N-T corneal thickness and TA<sub>3 mm</sub>, vectors  $J_0$  and  $J_{45}$ , or HOA<sub>3 mm</sub>, HOA<sub>6 mm</sub> in each group.

#### 4 Discussion

In the normal population, the corneal thickness of the superior, inferior, nasal, and temporal at the same distance from the corneal apex is inconsistent, superior>nasal>inferior>temporal. At different distances from the corneal apex, there is a regular increase in thickness. The peripheral 6 mm diameter concentric circle is thicker than the central thickness by 11% to 19% (Khoramnia et al., 2007). Therefore, when preparing the graft and bed, the different directions and the different center positions will affect the postoperative corneal thickness distribution. Our study of patients with keratoconus after FBDALK found that the S-I<sub>6 mm</sub> and N-T<sub>6 mm</sub> were 47.45 and 39.23 μm, respectively. Khoramnia et al. (2007) used Pentacam examination and found that in the normal population, the S-I<sub>6 mm</sub> and N-T<sub>6 mm</sub> were 34.01 and 16.79 μm, respectively; Zheng et al. (2008) reported those were 29.8 and 18.8 μm, respectively, which were significantly lower than those reported in our study. It indicated that corneal thickness in patients with keratoconus after FBDALK had significantly uneven distribution. The reasons included: (1) whether the peripheral cornea is involved during conic

expansion; (2) whether the central position of the bed creation is based on the pupillary center, the central cornea, or the expanded conical center; (3) whether the center of donor graft creation is based on the pupil center or the cornea apex; (4) whether the center, horizontal, and vertical positions of the bed are aligned with the center, horizontal, and vertical positions of the graft, respectively. The subjects in this study were keratoconic eyes, the base of cone did not exceed central 6 mm, and patients with the corneal expansion to the peripheral regions had been excluded. Therefore, the main influencing factors are the location of the center and the position of the graft-bed alignment. Intraoperatively, the preparation of bed and graft was centered with the pupillary center assessed by the naked eye under microscope, which might deviate from the actual pupillary center. Different pupil sizes might also affect the center positioning. The other influencing factors may be the inaccurate indication of the center of the graft and its horizontal or vertical directions. When the donor is placed during surgery, there might be some deviations between the center, horizontal, vertical positions of the graft and the center, horizontal, vertical positions of the bed. These factors would result in uneven distribution of postoperative corneal thickness.

In this study, the average pupillary center distance from the corneal apex was  $(0.47 \pm 0.23)$  mm, of which 10 eyes were located at 0.6 mm diameter outside the corneal apex. It was reported that in 81.7%–97.7% of the normal population, the pupillary center is often located inferior to the corneal apex at the temporal region at a certain distance. Ashwin et al. (2009) and Fares et al. (2012a) used Pentacam examination and found that in the normal population the pupillary center is located in the corneal apex of 0.6 mm diameter concentric circles. The deviation of the corneal apex from the pupillary center would affect postoperative visual quality. Our study showed the  $X$ -axis distance from corneal apex to the corneal pupillary center had a significant positive correlation with corneal astigmatism vector  $J_{45}$ .

The  $S-I_{2\text{ mm}}$  in this study was significantly and positively correlated with corneal astigmatism vectors  $J_0$  and  $J_{45}$  and total corneal HOA. The  $S-I_{4\text{ mm}}$  and  $S-I_{8\text{ mm}}$  were also significantly positively correlated with total corneal HOA. The results indicated that the uneven distribution of corneal thickness, especially at the pupil zone, might significantly affect the postop-

erative refractive status of patients. The reason is that the mechanical angular deformation will be induced by uneven distribution of the corneal biomechanical properties because of the uneven distribution of corneal thickness. This angular deformation will lead to astigmatism, possibly even high astigmatism or irregular astigmatism. The biomechanical properties of the cornea mainly depend on the characteristics of the matrix collagen fibers, including the number of collagen fibers in different arrangement directions, and the super-elasticity and anisotropy of collagen fibers. Via the  $X$ -ray scattering mode, it was found that the corneal stromal fiber had obvious characteristics. Approximately 66% of the lamellae are located in the nasal-temporal (horizontal) and superior-inferior (vertical) regions within  $45^\circ$ , while the remaining 33% are randomly oriented and the corneal collagen fibers are additionally strengthened in both the nasal-temporal and superior-inferior directions (Daxer and Fratzl, 1997; Boote et al., 2004; Pandolfi and Holzapfel, 2008; Petsche et al., 2012). At the center of the cornea, fibers are mainly in horizontal and vertical directions. If a variety of factors cause the central cornea regions, especially the number and the direction of horizontal and vertical fiber layers to be inconsistent, this will lead to variations in stress-strain properties of the corneal materials at different positions. However, in this study, there was no statistically significant correlation between nasal-temporal corneal thickness difference and corneal astigmatism, vectors  $J_0$ ,  $J_{45}$ , and total corneal HOA. This might be due to the fact that the corneal thickness difference did not reach a specific value sufficient to cause significant refractive changes. This needs further investigation.

## 5 Conclusions

Patients with advanced keratoconus after FBDALK have uneven distribution of corneal thickness at pupil zone and deviation of the corneal apex from the pupillary center. This might cause significant astigmatism, including regular and irregular astigmatism, and affect postoperative visual quality.

## Compliance with ethics guidelines

Bing-hong WANG, Ye-sheng XU, Wen-jia XIE, and Yu-feng YAO declare that they have no conflict of interest.

All procedures followed were in accordance with the ethical standards of the responsible committee on human

experimentation (institutional and national) and with the Helsinki Declaration of 1975, as revised in 2008 (5). Informed consent was obtained from all patients for being included in the study.

## References

- Ashwin PT, Shah S, Pushpott S, et al., 2009. The relationship of Central Corneal Thickness (CCT) to Thinnest Central Cornea (TCC) in healthy adults. *Cont Lens Anterior Eye*, 32(2):64-67.  
<https://doi.org/10.1016/j.clae.2008.07.006>
- Bae GH, Kim JR, Kim CH, et al., 2014. Corneal topographic and tomographic analysis of fellow eyes in unilateral keratoconus patients using Pentacam. *Am J Ophthalmol*, 157(1):103-109.e1.  
<https://doi.org/10.1016/j.ajo.2013.08.014>
- Bonci P, Della Valle V, Bonci P, et al., 2011. Deep anterior lamellar keratoplasty with dehydrated, 4 °C-stored, and rehydrated lenticules. *Eur J Ophthalmol*, 21(4):368-373.  
<https://doi.org/10.5301/EJO.2010.5972>
- Boote C, Dennis S, Meek K, 2004. Spatial mapping of collagen fibril organisation in primate cornea—an X-ray diffraction investigation. *J Struct Biol*, 146(3):359-367.  
<https://doi.org/10.1016/j.jsb.2003.12.009>
- Daxer A, Fratzl P, 1997. Collagen fibril orientation in the human corneal stroma and its implication in keratoconus. *Invest Ophthalmol Vis Sci*, 38(1):121-129.
- Espandar L, Mandell JB, Niknam S, 2016. Femtosecond laser-assisted decagonal deep anterior lamellar keratoplasty. *Can J Ophthalmol*, 51(2):67-70.  
<https://doi.org/10.1016/j.jcjo.2015.12.001>
- Fares U, Otri AM, Al-Aqaba MA, et al., 2012a. Correlation of central and peripheral corneal thickness in healthy corneas. *Cont Lens Anterior Eye*, 35(1):39-45.  
<https://doi.org/10.1016/j.clae.2011.07.004>
- Fares U, Sarhan ARS, Dua HS, 2012b. Management of post-keratoplasty astigmatism. *J Cataract Refract Surg*, 38(11):2029-2039.  
<https://doi.org/10.1016/j.jcrs.2012.09.002>
- Javadi MA, Motlagh BF, Jafarinabab MR, et al., 2005. Outcomes of penetrating keratoplasty in keratoconus. *Cornea*, 24(8):941-946.  
<https://doi.org/10.1097/01.ico.0000159730.45177.cd>
- Javadi MA, Feizi S, Rastegarpour A, 2011. Effect of vitreous length and trephine size disparity on post-DALK refractive status. *Cornea*, 30(4):419-423.  
<https://doi.org/10.1097/ICO.0b013e3181d4f8ff>
- Javadi MA, Feizi S, Javadi F, et al., 2014. Deep anterior lamellar keratoplasty using fresh versus cryopreserved corneas. *Ophthalmology*, 121(2):610-611.  
<https://doi.org/10.1016/j.ophtha.2013.10.007>
- Khoramnia R, Rabsilber TM, Auffarth GU, 2007. Central and peripheral pachymetry measurements according to age using the Pentacam rotating Scheimpflug camera. *J Cataract Refract Surg*, 33(5):830-836.  
<https://doi.org/10.1016/j.jcrs.2006.12.025>
- Nam SM, Im CY, Lee HK, et al., 2010. Accuracy of RTVue optical coherence tomography, Pentacam, and ultrasonic pachymetry for the measurement of central corneal thickness. *Ophthalmology*, 117(11):2096-2103.  
<https://doi.org/10.1016/j.ophtha.2010.03.002>
- Özyol P, Özyol E, 2016. Agreement between swept-source optical biometry and scheimpflug-based topography measurements of anterior segment parameters. *Am J Ophthalmol*, 169:73-78.  
<https://doi.org/10.1016/j.ajo.2016.06.020>
- Pandolfi A, Holzapfel GA, 2008. Three-dimensional modeling and computational analysis of the human cornea considering distributed collagen fibril orientations. *J Biomech Eng*, 130(6):061006.  
<https://doi.org/10.1115/1.2982251>
- Petsche SJ, Chernyak D, Martiz J, et al., 2012. Depth-dependent transverse shear properties of the human corneal stroma. *Invest Ophthalmol Vis Sci*, 53(2):873-880.  
<https://doi.org/10.1167/iov.11-8611>
- Ponce CMP, Rocha KM, Smith SD, et al., 2009. Central and peripheral corneal thickness measured with optical coherence tomography, Scheimpflug imaging, and ultrasound pachymetry in normal, keratoconus-suspect, and post-laser *in situ* keratomileusis eyes. *J Cataract Refract Surg*, 35(6):1055-1062.  
<https://doi.org/10.1016/j.jcrs.2009.01.022>
- Sarhan ARS, Dua HS, Beach M, 2000. Effect of disagreement between refractive, keratometric, and topographic determination of astigmatic axis on suture removal after penetrating keratoplasty. *Br J Ophthalmol*, 84(8):837-841.  
<https://doi.org/10.1136/bjo.84.8.837>
- Serdarevic ON, 1994. Refractive corneal transplantation: control of astigmatism and ametropia during penetrating keratoplasty. *Int Ophthalmol Clin*, 34(4):13-33.
- Shankar H, Taranath D, Santhirathelagan CT, et al., 2008. Anterior segment biometry with the Pentacam: comprehensive assessment of repeatability of automated measurements. *J Cataract Refract Surg*, 34(1):103-113.  
<https://doi.org/10.1016/j.jcrs.2007.09.013>
- Uçakhan ÖÖ, Özkan M, Kanpolat A, 2006. Corneal thickness measurements in normal and keratoconic eyes: Pentacam comprehensive eye scanner versus noncontact specular microscopy and ultrasound pachymetry. *J Cataract Refract Surg*, 32(6):970-977.  
<https://doi.org/10.1016/j.jcrs.2006.02.037>
- Vajpayee RB, Sharma V, Sharma N, et al., 2001. Evaluation of techniques of single continuous suturing in penetrating keratoplasty. *Br J Ophthalmol*, 85(2):134-138.  
<http://doi.org/10.1136/bjo.85.2.134>
- Wu SQ, Zhou P, Zhang B, et al., 2012. Long-term comparison of full-bed deep lamellar keratoplasty with penetrating keratoplasty in treating corneal leucoma caused by herpes simplex keratitis. *Am J Ophthalmol*, 153(2):291-299.e2.  
<https://doi.org/10.1016/j.ajo.2011.07.020>
- Yao YF, 2008. A novel technique for performing full-bed deep lamellar keratoplasty. *Cornea*, 27(Suppl 1):S19-S24.  
<https://doi.org/10.1097/ICO.0b013e31817f445f>
- Yao YF, Zhang B, Zhou P, et al., 2002. Autologous limbal

- grafting combined with deep lamellar keratoplasty in unilateral eye with severe chemical or thermal burn at late stage. *Ophthalmology*, 109(11):2011-2017.  
[https://doi.org/10.1016/S0161-6420\(02\)01258-7](https://doi.org/10.1016/S0161-6420(02)01258-7)
- Zhang YM, Wu SQ, Yao YF, 2013. Long-term comparison of full-bed deep anterior lamellar keratoplasty and penetrating keratoplasty in treating keratoconus. *J Zhejiang Univ-Sci B (Biomed & Biotechnol)*, 14(5):438-450.  
<https://doi.org/10.1631/jzus.B1200272>
- Zheng YF, Huang GF, Huang WY, et al., 2008. Distribution of central and peripheral corneal thickness in Chinese children and adults: the Guangzhou twin eye study. *Cornea*, 27(7):776-781.  
<https://doi.org/10.1097/ICO.0b013e31816f62d3>

## 中文摘要

题 目：全植床深板层角膜移植术后角膜厚度的分布及顶点的位置对术后屈光状态的影响

**目 的：**探讨全植床深板层角膜移植术后角膜厚度的分布及顶点的位置对术后屈光状态的影响。

**创新点：**角膜移植术后的高度散光或不规则散光都会严重影响患者的术后视力，部分患者甚至成为无法矫正的低视力。角膜移植术后植片和植床厚度的偏倚及顶点位置的偏倚可能会导致明显散光，目前并没有相关的研究报道。

**方 法：**回顾性分析相关病例，严格纳入标准，记录进展期圆锥角膜的患者全植床深板层角膜移植术后的裸眼视力、最佳矫正视力及 Pentacam 检查结果，包括各个区域的角膜厚度差值、角膜瞳孔中心距角膜顶点的距离及散光矢量值、高阶像差，进行相关数据分析。

**结 论：**进展期圆锥角膜的患者经全植床深板层角膜移植术后，角膜瞳孔区厚度分布的不均匀及角膜顶点偏离瞳孔中心，都可能会造成明显散光，包括规则和不规则散光，从而影响术后的视觉效果。

**关键词：**全植床深板层角膜移植；角膜厚度分布；角膜顶点